Project Report
ATC-376

Convective Weather Avoidance Modeling for Low-Altitude Routes

S.E. Campbell
R.A. DeLaura

31 May 2011

Lincoln Laboratory
MASSACHUSETTS INSTITUTE OF TECHNOLOGY
LEXINGTON, MASSACHUSETTS

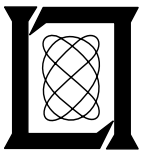

Prepared for the Federal Aviation Administration,
Washington, D.C. 20591

1. Report No.	2. Government Accession No.	3. Recipient's Catalog No.
ATC-376		

4. Title and Subtitle	5. Report Date
Convective Weather Avoidance Modeling for Low-Altitude Routes	31 May 2011
	6. Performing Organization Code

7. Author(s)	8. Performing Organization Report No.
Scot Campbell and Richard DeLaura, Group 43	ATC-376

9. Performing Organization Name and Address	10. Work Unit No. (TRAIS)
MIT Lincoln Laboratory 244 Wood Street Lexington, MA 02420-9108	11. Contract or Grant No. FA8721-05-C-0002

12. Sponsoring Agency Name and Address	13. Type of Report and Period Covered
Department of Transportation Federal Aviation Administration 800 Independence Ave., S.W. Washington, DC 20591	Project Report
	14. Sponsoring Agency Code

15. Supplementary Notes

This report is based on studies performed at Lincoln Laboratory, a center for research operated by Massachusetts Institute of Technology, under Air Force Contract FA8721-05-C-0002.

16. Abstract

Thunderstorms are a leading cause of delay in the National Airspace System (NAS), and significant research has been conducted to predict the areas pilots will avoid during a storm. An example of such research is the Convective Weather Avoidance Model (CWAM), which provides the likelihood of pilot deviation due to convective weather in a given area. This report extends the scope of CWAM to include low-altitude flights, which typically occur below the tops of convective weather and have slightly different operational constraints. In general, the set of low-altitude flights includes short-hop routes and low-altitude escape routes used to reduce the impact of convective weather in the terminal area. For classification, low-altitude flights are identified as either deviations or non-deviations, and the corresponding weather features are analyzed. Precipitation intensity is observed to be the best predictor of deviation in the low-altitude flight regime, as compared to the difference in altitude between the flight and the echo tops for en route flights. Additionally, the low-altitude CWAM performs better than the departure CWAM currently used in the Route Availability Planning Tool (RAPT) when tested on deterministic weather data.

17. Key Words	18. Distribution Statement
	This document is available to the public through the National Technical Information Service, Springfield, VA 22161.

19. Security Classif. (of this report)	20. Security Classif. (of this page)	21. No. of Pages	22. Price
Unclassified	Unclassified	33	

This page intentionally left blank.

TABLE OF CONTENTS

This page intentionally left blank.

LIST OF ILLUSTRATIONS

This page intentionally left blank.

LIST OF TABLES

This page intentionally left blank.

1. INTRODUCTION

Convective weather is a significant impediment to effective and efficient Air Traffic Management (ATM) decisions, and sometimes results in unnecessary delays to the National Airspace System (NAS). 70% of delays in the NAS are caused by weather, and of those delays, 60% are specifically accounted for by convective weather [1]. Currently, rerouting decisions made by air traffic managers are aided by weather products such as the Corridor Integrated Weather System (CIWS) and the National Convective Weather Forecast (NCWF) [2, 3]. While these products provide a high quality representation of storm activity, it is difficult to predict the NAS impact from data based solely on the weather. In a Next Generation ATM system, decision support tools such as the Route Availability Planning Tool (RAPT) will mitigate weather-induced delays by supplementing the situational awareness of an air traffic manager with a forecast of the availability of specific flight routes [4]. The RAPT tool is based on the Convective Weather Avoidance Model (CWAM), which is a probabilistic model of pilot decision making in the presence of convective weather [5]. The output of CWAM is a three dimensional weather avoidance field (WAF), which is a probability map of the likelihood that a pilot will deviate at a specific position and time given the current and forecasted weather.

CWAM was originally developed for the en route flight regime by correlating observed weather with trajectories of aircraft that penetrated or avoided areas of convective weather. The deviation decision of each flight was recorded, and the weather statistics for each route were obtained using data from CIWS and stored in a database. Deviations were determined by comparing the distance between the actual and planned trajectories of the flight, and if that distance was greater than a specified "deviation threshold," a deviation was recorded. Pattern classification experiments were run on the CWAM database and the results showed that the most descriptive predictors for deviation were related to the echo top height, where the most descriptive was the difference in altitude between the aircraft and the echo top height [5]. In the terminal area, several studies of the Dallas and Memphis areas using weather information from the Integrated Terminal Weather System (ITWS) showed that deviation decisions are more closely related to the radar intensity of the storm and the proximity of the aircraft to the airport [6, 7].

This report presents the development of a low altitude version of CWAM which is based on a database composed of weather encounters that occur during level flight at or below FL240. The low altitude CWAM described here is applicable to jet traffic that uses low altitude air routes to 'escape' from terminal areas when weather or volume congestion impacts lead to constraints on high altitude airspace, or to low altitude flight by regional jets on 'short hop' routes. Such traffic was commonly observed in the New York metroplex as part of the field evaluation of RAPT. The creation of a low altitude CWAM will enable RAPT to provide weather impact guidance on low altitude routes that are currently excluded from the RAPT departure route database.

For this study, flight trajectories are obtained from the Enhanced Traffic Management System (ETMS) database, and weather data are acquired from CIWS for nine convective weather days across two

geographical regions (Chicago and New York). A Gaussian classifier is used to determine a set of deviation predictors and the results are tested on observed data. The predictor performance is compared to the existing terminal departure CWAM used in RAPT, and the differences are discussed.

2. METHODS

The database for this work reflects the behavior of low altitude flight deviations in the presence of convective weather. A low altitude flight is defined as a flight which achieves level flight below FL240, and does not climb above FL240 within 20 minutes of departure. Extremely low altitude flights (< 10 kft) and flights involving light aircraft are excluded from the database. Additionally, flights that make a decision to deviate while climbing or descending are not included in the database. The database contains an entry for each flight, and includes statistics on the type and severity of weather encountered as well as whether or not the flight deviated.

Flight trajectories are obtained from the ETMS database for a set of days involving convective weather in the Chicago and New York areas. The ETMS data provide the three dimensional position of each flight (with a 1 minute time step), and a list of navigation fixes that represent the flight plan of each flight. Weather data are acquired from the CIWS archive, and weather characteristic fields were created and used as deviation predictors. The details of the weather characteristic fields are described later in this section.

There are two categories of flight observed in the set of low altitude flights. First, and most prominent, are short haul routes where the cruise altitude of the aircraft does not pass above FL240. The second category involves a step climb where the aircraft levels off below FL240 before resuming its climb to cruise. Typically, the step climb routes encounter weather closer to the airport than the short haul routes.

The original CWAM used an automated process to separate deviations from non-deviations by comparing the distance between the actual and planned trajectories of a flight to a “deviation threshold.” In the en route environment this is an acceptable strategy because flights rarely stray from their planned route. In the low altitude environment this is not the case as aircraft are routinely vectored for shortcuts (predominately short haul routes), or traffic in the terminal area (step climb routes). Figure 1 illustrates a case in which the flight did not follow the planned route.

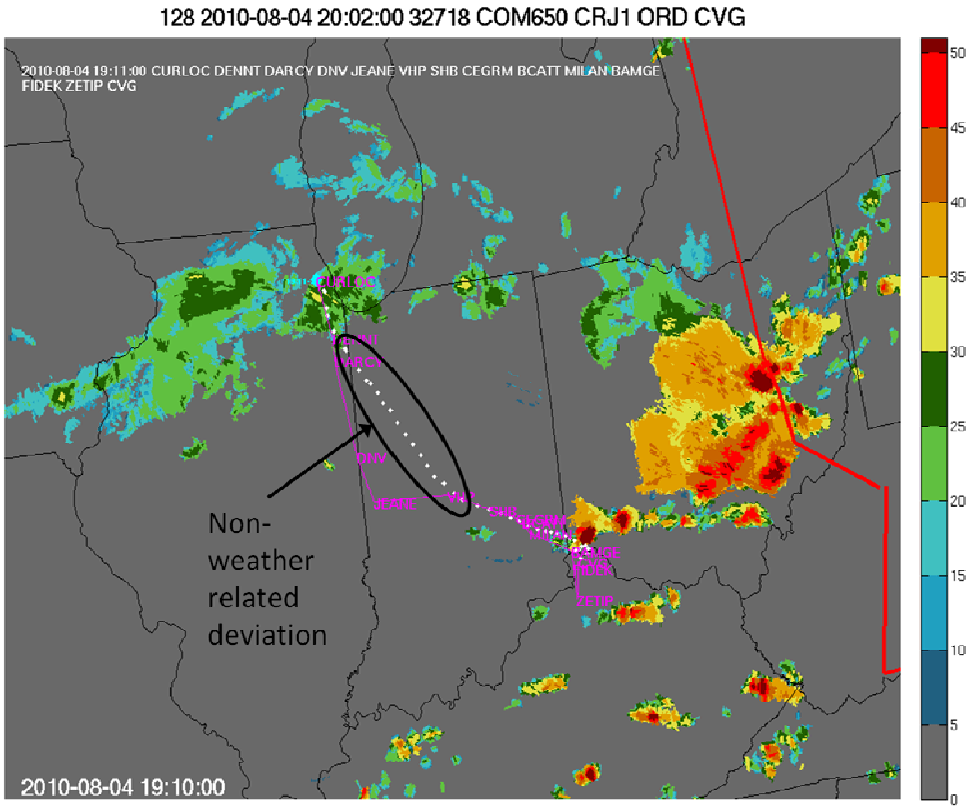

Figure 1. Example of low altitude flight not following planned route.

The magenta line shows the planned route and the white dots show the actual trajectory. In this example, the flight originates from Chicago O'Hare International Airport (ORD) and changes its route soon after departure to take a more direct track to Cincinnati/Northern Kentucky International Airport (CVG). This is a common shortcut given by ATC, and whether it is given primarily depends on the density of traffic and other hazards to flight in the region. Because of these inconsistencies, an automated process to determine deviations is infeasible; therefore, each trajectory in the low altitude database is manually analyzed to determine whether or not it is a deviation. In the analysis, a deviation is recorded when a flight is observed to make a decisive maneuver to avoid weather while in level flight. Figure 2 shows a flight from Chicago to Cincinnati which deviates around weather.

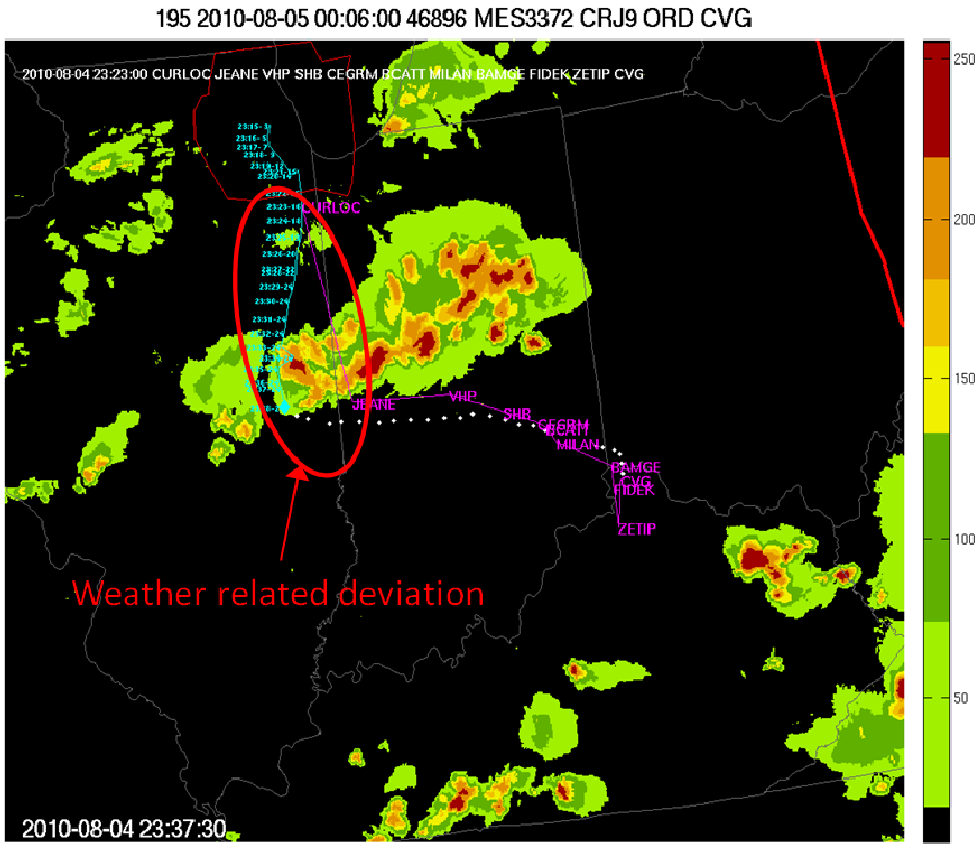

Figure 2. In-flight deviation around convective weather.

If a deviation is identified, the weather characteristics responsible for the deviation are recorded from the planned flight path at the time of the deviation decision. On the other hand, a non-deviation is recognized as a flight that penetrates weather with VIL ≥ 1 and does not deviate. In this case, the weather characteristics are recorded at the point along the flight path where the flight encountered the highest VIL. The low altitude database contains flights from nine days and two regions. The regions consist of Chicago and New York, and the airports are Chicago O'Hare (ORD), Midway (MDW), New York LaGuardia (LGA), John F. Kennedy (JFK), and Newark (EWR). Table 1 lists the number of deviations and non-deviations in each region on each day in the database. The total number of flights in the database is 2539, where 1248 of the flights encountered weather and 309 flights deviated because of the weather. It should be noted that "serial deviations," where a flight deviated more than once, are not recorded as multiple deviations. Additionally, weather encounters that occur before or after a deviation are not recorded as multiple encounters.

Table 1. Number of Trajectories in the Low Altitude CWAM Database

	ORD, MDW		JFK, LGA, EWR	
Date	**Deviations**	**Non-Deviations**	**Deviations**	**Non-Deviations**
06/08/2009	43	91	--	--
06/09/2009	--	--	34	133
06/13/2009	--	--	42	122
06/19/2009	33	64	--	--
08/10/2009	--	--	38	51
04/07/2010	23	117	--	--
06/01/2010	--	--	48	100
06/04/2010	17	101	--	--
08/04/2010	31	160	--	--
Total	147	533	162	406

Table 2 lists the weather characteristics which describe the possible weather metrics that could influence a pilot's decision to deviate around a storm. This list is based on intuition formed from previous work [4-7], and the available weather data. The kernel size is the side-length of the square spatial filter applied at each grid point of the data. For example, VIL8(x,y) is the 90th percentile VIL value in an 8×8 km square centered at the grid point (x,y). The variance characteristics are calculated over an 8 km kernel, and in the case of echo tops, the data are pre-processed to exclude values less than 30,000 ft.

Table 2. Set of Weather Characteristics

VIL1 (90th Percentile Precipitation Intensity, 1 km kernel)	VIL8 (90th Percentile Precipitation Intensity, 8 km kernel)	VIL16 (90th Percentile Precipitation Intensity, 16 km kernel)
ET1 (90th Percentile Echo Top Height, 1 km kernel)	ET8 (90th Percentile Echo Top Height, 8 km kernel)	ET16 (90th Percentile Echo Top Height, 16 km kernel)
VILVAR (90th Percentile VIL Variance, 8 km kernel)	ETVAR (90th Percentile Echo Top Height Variance, 8 km kernel)	VILCOV (Area Percent Coverage with VIL ≥ 3, 16 km kernel)
VILpVAR (VIL1 + Maximum VIL Variance, 8 km kernel)	ETpVAR (ET1 + Maximum Echo Top Height Variance, 8 km kernel)	

The creation of the VILpVAR and ETpVAR weather characteristics is motivated by recent work that found stratiform rain to be a common false deviation prediction error mode in CWAM [8]. A characteristic of stratiform rain is intense precipitation with high cloud tops over a large area, which results in a WAF with high probability of deviation. However, in spite of the high WAF values, aircraft are frequently observed flying through these regions. A more implicit characteristic of stratiform rain is a low variance in VIL and echo tops across the area, and these are the properties exploited in VILpVAR and ETpVAR. For example, VILpVAR is the sum of the VIL at a grid point and the maximum variance of VIL in an 8 km kernel around that grid point. Stratiform rain results in a large VIL value with a small variance in VIL which drives VILpVAR to be lower compared to a normal convective cell (which has large VIL with a large variance in VIL). This gives the appearance that stratiform rain is less dangerous than regular convection. Figure 3 illustrates this point by showing a flight through stratiform rain over Chicago. The figures on the left side show the VIL and echo tops of the system, which are as high as level 5 and 40,000 ft, respectively. The figure on the right shows the same flight overlaid on VILpVAR, which is much more benign and shows the flight going through an equivalent level 2 of precipitation.

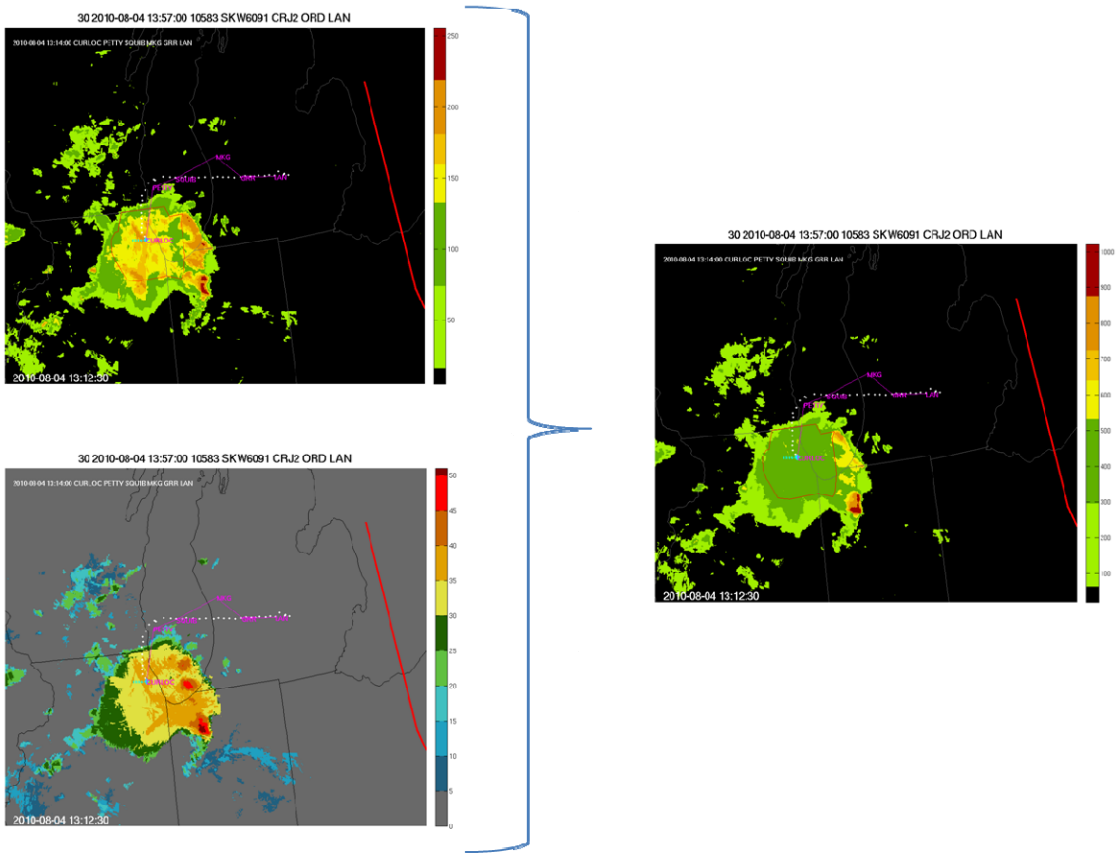

Figure 3. A flight through stratiform rain over Chicago. Left top: Flight overlaid on VIL. Left bottom: Flight overlaid on echo tops. Right: Flight overlaid on VILpVAR.

The low altitude deviation database is input to a Gaussian classifier that uses a diagonal covariance matrix and a linear discriminant function. This is the same technique used in previous work [5]. The classifier finds the combination of predictors that minimize the overall classification error. In addition, it finds the corresponding separating hyperplane that defines the boundary between the deviation and non-deviation spaces. The output from the classification experiment is a set of "best" predictors and combinations of predictors that are used in a series of modeling experiments to confirm their relative performance. The database was partitioned into histogram bins defined for the set of predictors, and the observed probability of deviation was found for each bin. The probability of deviation bins were filled out and smoothed using a discretized smoothing spline technique based on the discrete cosine transform [9]. The resulting smoothed tables were tested as candidate WAFs, and the performance of the predictors were compared.

3. RESULTS

Figure 4 compares the total prediction error for several combinations of the predictors, where the total prediction error is the percentage of incorrect predictions in the set of encounters contained in the database.

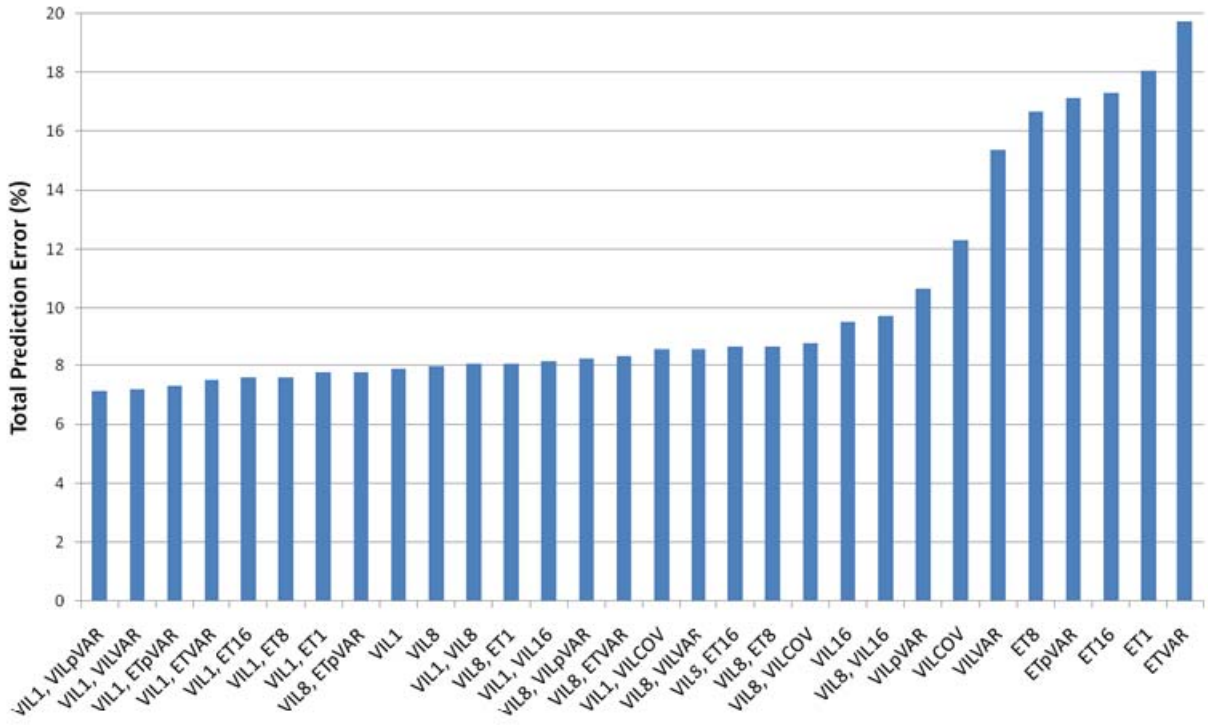

Figure 4. Total predictor error of the full set of 1- and 2-predictor classifiers.

According to Figure 4, VIL is the dominant predictor in the set of weather characteristics. The most accurate predictor is {VIL1, VILpVAR}, which also shows the benefit of accounting for the variance of the VIL to better detect areas of stratiform rain. However, there is little difference in total prediction error when the 1-predictor VIL classifiers are compared to the 2-predictor classifiers. This implies little benefit to the addition of a second predictor to the classifier. In addition, echo tops are shown to be not a good predictor of deviation for low altitude routes, which confirms previous that claimed precipitation intensity to be the best predictor in the terminal area [6, 7].

To better understand the relative differences between multi-predictor classifiers with similar total prediction error rates, a "best" classifier is selected from each of the N-predictor classifiers and their results are compared. Figure 5 lists the "best" predictor(s) for each N-predictor classifier and shows the total prediction error for the full dataset as well as for the specific datasets of Chicago and New York. The total prediction error for the complete dataset, Chicago, and New York are given as the green, blue, and red squares, respectively.

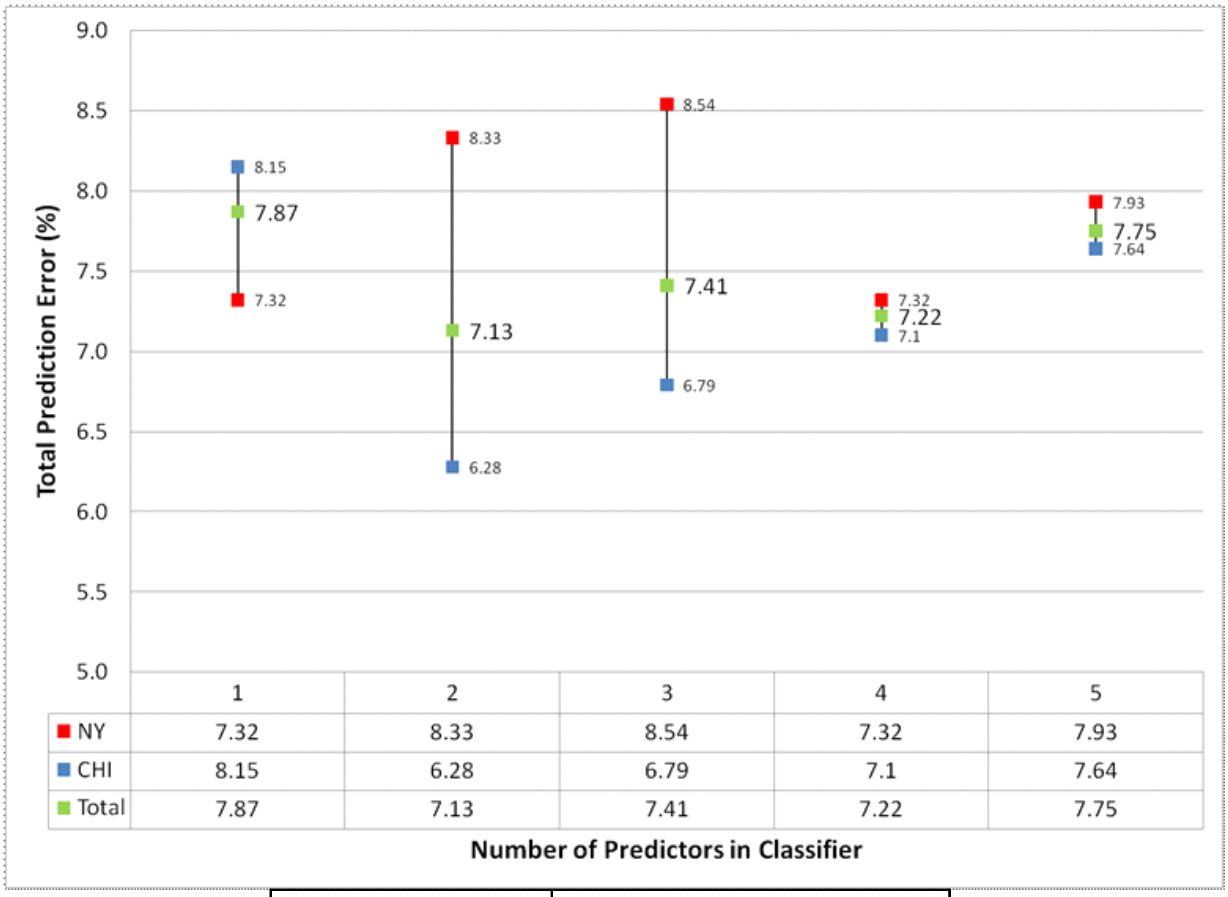

	1	2	3	4	5
NY	7.32	8.33	8.54	7.32	7.93
CHI	8.15	6.28	6.79	7.1	7.64
Total	7.87	7.13	7.41	7.22	7.75

1 Predictor	VIL1
2 Predictor	VIL1, VILpVAR
3 Predictor	VIL1, VILpVAR, ETVAR
4 Predictor	VIL1, VILpVAR, VIL8, ET1
5 Predictor	VIL1, VILpVAR, VIL8, ET1, ET16

Figure 5. Comparison of total prediction error between different geographic regions and classifiers with different number of predictors.

In general, as the number of predictors increases, the total prediction error of the full dataset does not change significantly. However, it is interesting that the 4- and 5-predictor classifiers result in a much smaller spread in error between Chicago and New York than the lower-order predictor classifiers. Additionally, although the addition of VILpVAR to the 1-predictor classifier results in lower total prediction error, the spread in error between Chicago and New York increases dramatically. Also, the total error in Chicago is much less than the error in New York, which indicates VILpVAR does a good job in handling stratiform rain (more prevalent in the Chicago dataset), but is not very adaptable to other scenarios. Another explanation is that there could be more high-topped anvil cases in New York than Chicago, which VILpVAR would incorrectly score as non-deviation regions.

It is equally important to consider deviation and non-deviation error in addition to total prediction error when investigating the performance of a classifier. Deviation error is defined as the number of misclassified deviations divided by the number of deviations, and non-deviation error is defined as the number of misclassified non-deviations divided by the number of non-deviations. The relationship between deviation and non-deviation error provides insight into whether the classifier is under or over-predicting deviations. In many cases, two classifiers can have similar total prediction error but vastly different deviation or non-deviation errors. Figure 6 compares the total prediction error, deviation error, and non-deviation error for the set of classifiers shown in Figure 5. The spread between the deviation and non-deviation errors increases between the 1- and 2-predictor classifiers, but decreases with the 3-predictor classifier. The addition of 4- and 5-predictors does not significantly affect the total error or the deviation/non-deviation error spread. This is a similar behavior as has been observed previously [5].

Although there is a slight decrease in total predictor error for a multi-predictor classifier compared to a 1-predictor classifier, it is not enough to justify the associated increase in complexity and error spread. Therefore, 1-predictor classifiers (VIL1, VIL8, and VIL16) were tested against the data to gain further understanding of their performance. Figure 7 presents the smoothed probability of deviation tables for the 1-predictor classifiers.

Weather encounters are divided into 10 bins based on the value of VIL (0-255) as determined by each model's spatial filter. The probability of deviation is calculated by the ratio of deviations to non-deviations inside each bin. In Figure 7, the vertical lines show the partitions of the 6-level VIP scale, and the color indicates the probability of deviation.

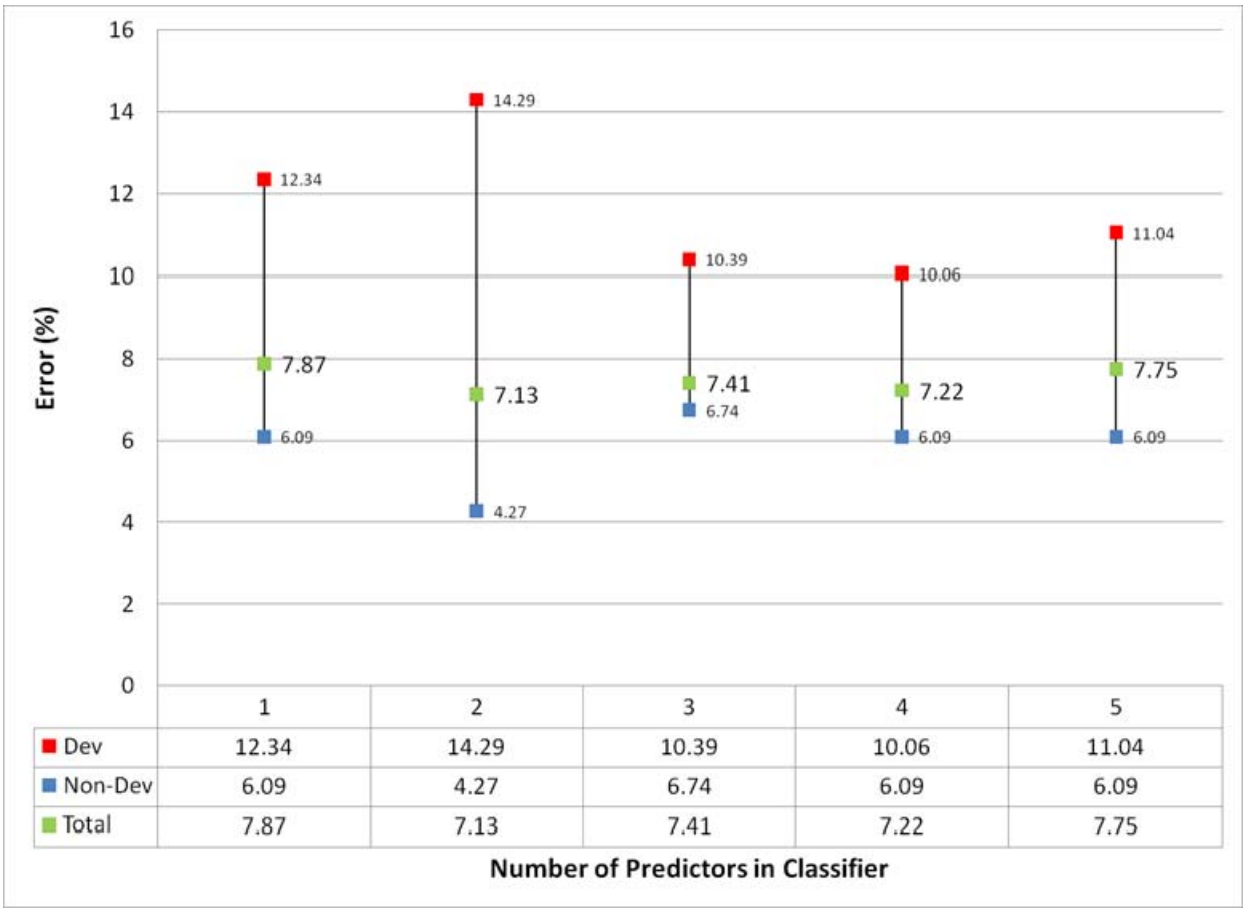

Figure 6. Comparison of total prediction error, deviation error, and non-deviation error for classifiers with different numbers of predictors.

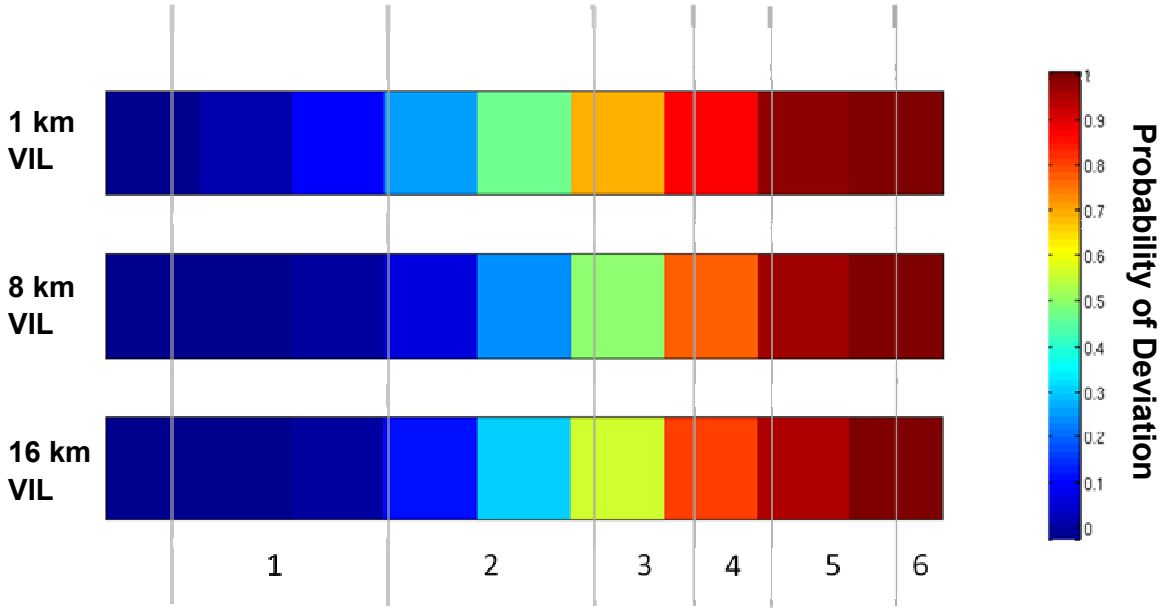

Figure 7. WAF lookup table for three 1-predictor models with different spatial filter size.

Figure 8 shows deviation/non-deviation histograms for the low altitude database using the three spatial filters described above. The top figure uses the native 1 km VIL resolution, the middle figure uses an 8 km spatial filter, and the bottom figure uses a 16 km spatial filter. At first glance there is not much difference between the histograms. But a detailed analysis reveals that as the size of the spatial filter increases, the number of non-deviations at each VIP level increases, whereas the number of deviations at each VIP level remains relatively unchanged. It makes sense that the number of non-deviations increases with spatial filter size because the filter grows the physical size of the weather regions, causing a flight that might be a non-encounter with the 1 km resolution to be a non-deviation with the 8 km spatial filter. The fact that the number of deviations does not change much with spatial filter size implies that the flights, in general, do not deviate unless their proposed flight path passes through an area of severe weather. In other words, flights do not give much margin of safety between the storm and their flight plan. The behavior is also reflected in the total prediction error of the predictors, which increases with spatial filter size.

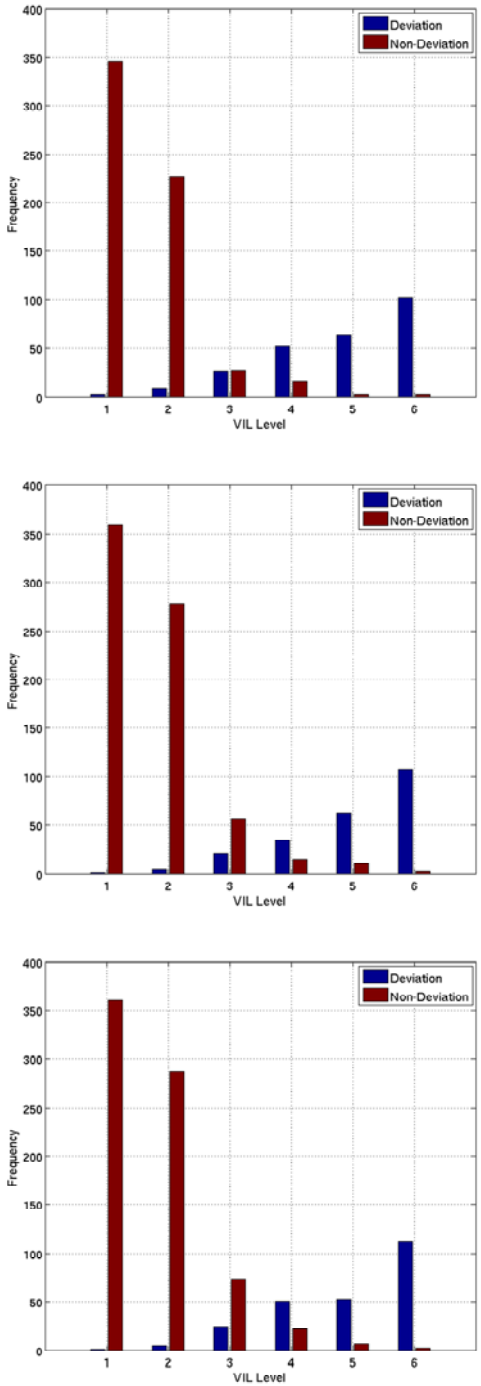

Figure 8. Deviation/non-deviation histograms. Top: 1 km spatial filter. Middle: 8 km spatial filter. Bottom: 16 km spatial filter.

Figure 9 shows the relative performance of the 1-predictor models and the existing terminal area departure WAF currently used in RAPT in terms of the probability of detection, false alarm rate, and critical skill index. The probability of detection (*PoD*) is shown in equation 1, where *hits* are correct predictions of deviation and *misses* are incorrect predictions of deviation.

$$PoD = \frac{hits}{hits + misses} \tag{1}$$

The false alarm rate (*FAR*) is given in equation 2, where *false* is the number of false predictions.

$$FAR = \frac{false}{hits + false} \tag{2}$$

The critical skill index (*CSI*) is a measure of the overall skill of the predictor and is given in equation 3.

$$CSI = \frac{hits}{hits + misses + false} \tag{3}$$

The red, blue, and black lines represent the performance of the model tested on the Chicago, New York, and combined databases, respectively. The green line shows the performance of the current departure WAF in RAPT when tested on the combined database. The most apparent observations from Figure 9 are the differences between the performance in Chicago and New York and the improvement in overall performance compared to the current RAPT departure WAF. It is interesting that the WAF threshold for maximum CSI is much lower for the RAPT departure WAF compared to the WAF models developed for this report. This implies that the RAPT departure WAF is under-predicting deviations in the low altitude flight regime. In other words, flights in the low altitude regime deviate around less severe weather than initially expected in the RAPT development. Additionally, the RAPT departure WAF does not perform as well in the tradeoff between probability of detection and false alarm rate. A good way to qualify the best tradeoff between probability of detection and false alarm rate is to see which data points are closest to the top left corner of the figure (PoD = 1.0, FAR = 0.0). All three predictors (VIL1, VIL8, VIL16) show a strong “kink” in the PoD vs. FAR curves which indicates there is a clear choice for the best WAF threshold.

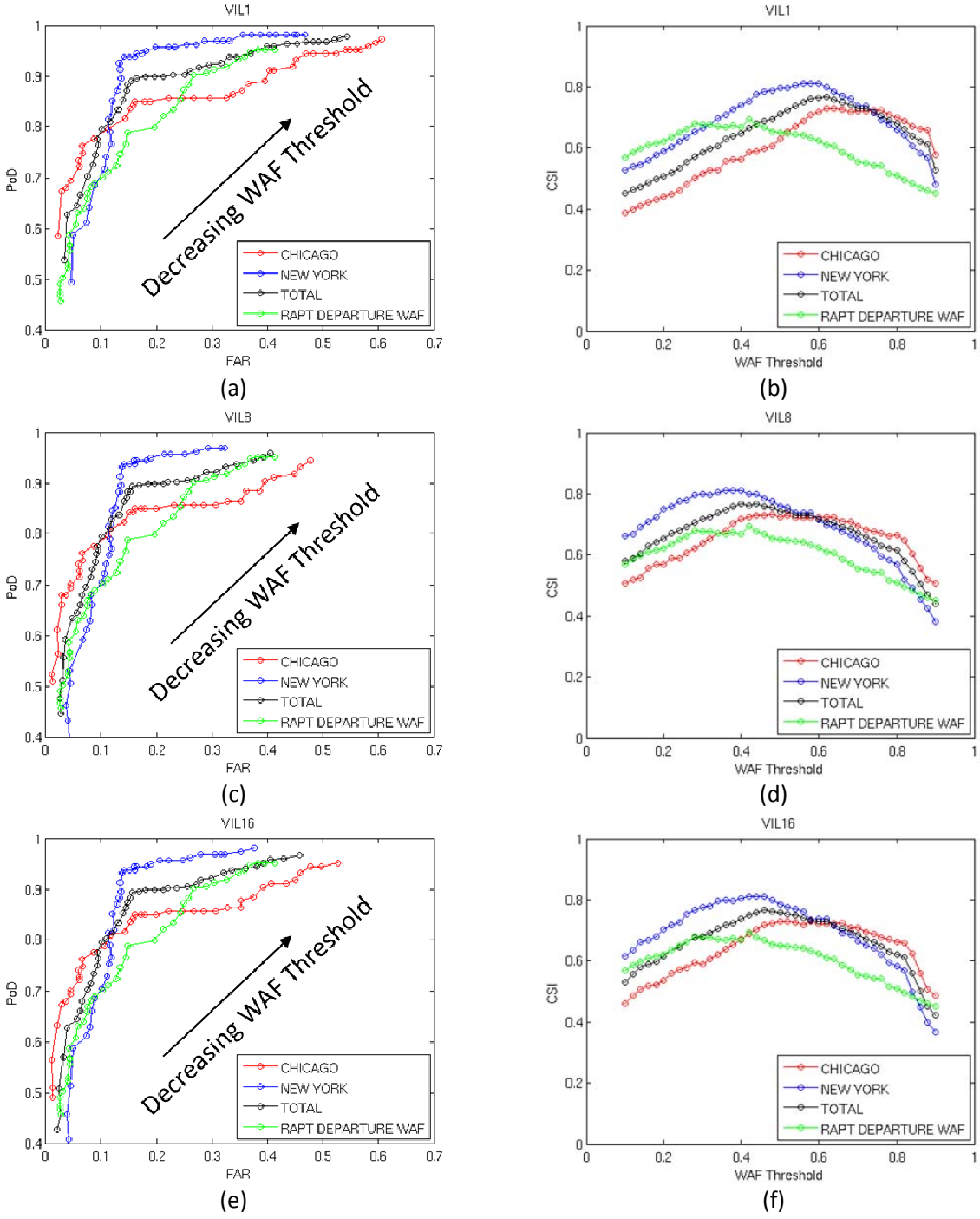

Figure 9. Predictor performance (probability of detection vs. false alarm rate and critical skill index vs. WAF threshold) for predictors of different spatial filter size. Top (a,b): 1 km kernel. Middle (c,d): 8 km kernel. Bottom (e,f): 16 km kernel.

The maximum CSI for the predictors is compared in Figure 10a. The maximum CSI scores for the VIL1, VIL8, and VIL16 predictors were almost identical, and they consistently performed better in New York than Chicago. The RAPT departure WAF is much more consistent between New York and Chicago, but shows worse overall performance when compared to the predictors developed in this report. Figure 10b shows the decisiveness ratio of the predictors, where the decisiveness ratio is the fraction of flights which encounter WAF values greater than 70% and less than 30%. The decisiveness ratio is calculated with equation 4, where $N_{enc>70\%}$ is the number of encounters which penetrate a WAF contour greater than 70%, $N_{enc<30\%}$ is the number of encounters which penetrate a WAF contour less than 30%, and N_{tot} is the total number of encounters.

$$Decisiveness\ Ratio = \frac{N_{enc>70\%} + N_{enc<30\%}}{N_{tot}} \tag{4}$$

Generally speaking, the deciciveness ratio gives a sense of the fraction of flights that can be identified as either a deviation or non-deviation at a high level of confidence.

The most decisive predictor is VIL8, followed by VIL16, VIL1, and lastly the RAPT departure WAF. Decisiveness is an important metric because it is a measure of the certainty of the predictor. For example, a highly certain predictor enhances situational awareness in ATM by providing "yes/no" advice on route blockage instead of "maybe."

In using this research to determine the best predictor for the low altitude dataset, one must consider decisiveness in addition to the prediction error and critical skill index. From the results of this work, VIL8 (VIL with an 8 km spatial filter) is the best combination of accuracy and decisiveness.

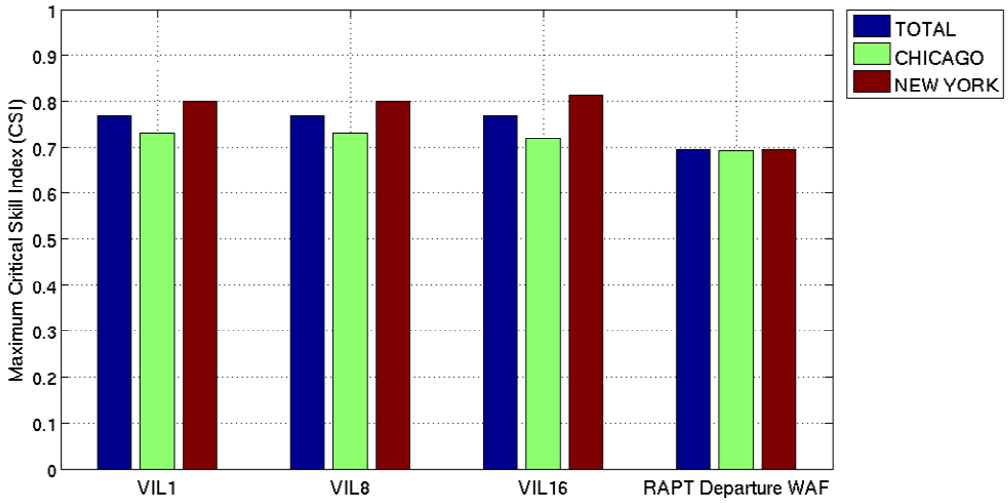

(a)

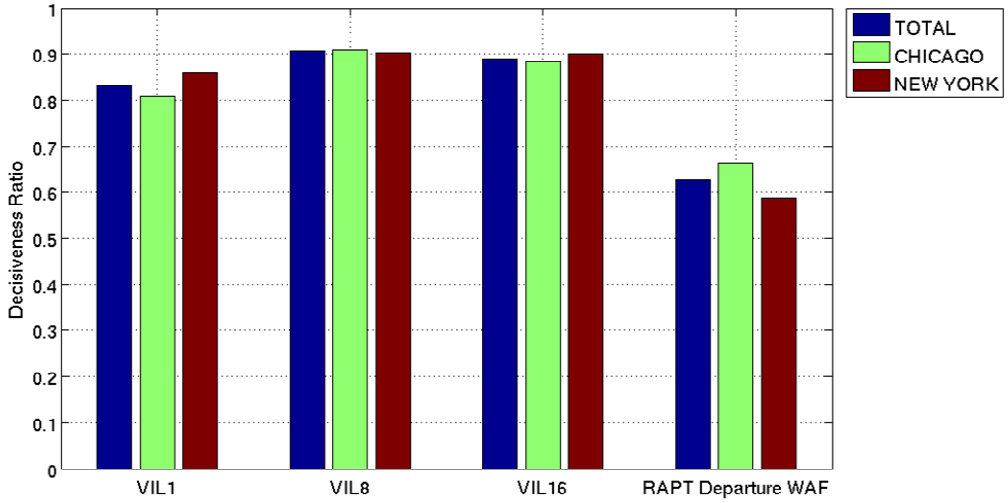

(b)

Figure 10. Comparison of maximum CSI (a) and decisiveness ratio (b) for the classifiers analyzed in this report.

4. CONCLUSIONS

This study introduces a low altitude version of CWAM, which is an extension of the existing CWAM which was developed for the en route flight regime. It presents a probabilistic model of pilot deviation decision making for flights at or below FL240 in the presence of convective weather. The model was applied to a database of nearly 1000 encounters with convective weather, of which 309 resulted in deviations. It was found that precipitation intensity, specifically VIL level, is the dominating predictor in the low altitude flight regime. Moreover, there is little added benefit to adding additional predictors to the VIL-based classifier model. Lastly, the low altitude CWAM developed by this work showed better performance in both accuracy and decisiveness than the current departure CWAM used in RAPT when tested on real data.

Future work should include an expansion of the low altitude database, which will allow a more robust analysis of the predictors to validate these results and give a better indication of the true performance of higher dimension classifiers. Additional work is needed to investigate the differences in performance between New York and Chicago airspace and to determine if there are significant airspace dependencies that can be identified and corrected for. More work should be done in refining the VILpVAR metric, as it showed promise in mitigating the effect of a common error mode (stratiform rain). It is also necessary to apply these models to a scenario involving forecasted weather to analyze the impact of the added uncertainty to the classifier performance. Finally, the low altitude route structure needs to be better defined in order to integrate this work with a tool such as RAPT.

This page intentionally left blank.

APPENDIX A
PREDICTION MODEL

The weather avoidance fields (WAFs) in the low altitude CWAM are generated with a prediction model that will be described in this appendix. The database of low altitude flights through convective weather includes weather statistics calculated from CIWS, and flight trajectories obtained from ETMS. Predictors of deviation are selected from a set of weather characteristics that are listed in Table A1.

Table A1. Set of Weather Characteristics

VIL1 (90^{th} Percentile Precipitation Intensity, 1 km kernel)	VIL8 (90^{th} Percentile recipitation Intensity, 8 km kernel)	VIL16 (90^{th} Percentile Precipitation Intensity, 16 km kernel)
ET1 (90^{th} Percentile Echo Top Height, 1 km kernel)	ET8 (90^{th} Percentile Echo Top Height, 8 km kernel)	ET16 (90^{th} Percentile Echo Top Height, 16 km kernel)
VILVAR (90^{th} Percentile VIL Variance, 8 km kernel)	ETVAR (90^{th} Percentile Echo Top Height Variance, 8 km kernel)	VILCOV (Area Percent Coverage with VIL ≥ 3, 16 km kernel)
VILpVAR (VIL1 + Maximum VIL Variance, 8 km kernel)	ETpVAR (ET1 + Maximum Echo Top Height Variance, 8 km kernel)	

The predictors are input to a classification experiment based on a Gaussian model with a diagonal covariance matrix and a linear discriminant function. The objective of the classification experiment is minimum total predication error, and the best predictor was found to be {VIL1, VILpVAR}, but with VIL playing a dominating role. Analysis of the classification results shows VIL alone to be a sufficient predictor of deviation, and three VIL models of different spatial filters are further analyzed in the report. One model uses the native resolution of VIL (1 km), and the other two models use spatial filters of 8 km, and 16 km, respectively. The spatial filter consists of a box with side-length (x)km surrounding the grid point in question, and the 90^{th} percentile of the VIL inside the box given as the filtered value at that grid point.

Probability of deviation tables for the three models are calculated by dividing the deviation/non-deviation database into 10 equally sized bins based on the model's filtered VIL values, and the probability of deviation inside of each bin is calculated with the ratio of deviations to non-deviations. The WAF tables for each model are found by smoothing the probability of deviation tables using a discretized smoothing spline technique based on the discrete cosine transform. The resulting tables are shown in Table A2.

Table A2. WAF Tables

VILrange	**0≤x≤25.5**	**25.5<x≤51**	**51<x≤76.5**	**76.5<x≤102**	**102<x≤127.5**
VIL1	0	0.02516	0.11111	0.27404	0.48051
VIL8	0.00133	0.00896	0.02204	0.08568	0.26515
VIL16	0.00133	0.00257	0.02416	0.12548	0.32801
VIL range	127.5<x≤153	153<x≤178.5	178.5<x≤204	204<x≤229.5	229.5<x≤255
VIL1	0.69443	0.87615	0.98004	1	1
VIL8	0.52951	0.80275	0.99382	1	1
VIL16	0.57795	0.81472	0.95162	1	1

GLOSSARY

ATC	Air Traffic Control
ATM	Air Traffic Management
CIWS	Corridor Integrated Weather System
CSI	critical skill index
CVG	Cincinnati/Northern Kentucky International Airport
CWAM	Convective Weather Avoidance Model
ETMS	Enhanced Traffic Management System
EWR	Newark Liberty International Airport
FAR	false alarm rate
ITWS	Integrated Terminal Weather System
JFK	John F. Kennedy Airport
LGA	New York LaGuardia Airport
MDW	Chicago Midway Airport
NAS	National Airspace System
NCWF	National Convective Weather Forecast
ORD	Chicago O'Hare International Airport
PoD	probability of detection
RAPT	Route Availability Planning Tool
VIL	Vertically Integrated Liquid Water
VIP	Video Integrator and Processor
WAF	weather avoidance field

This page intentionally left blank.

REFERENCES

[1] Clifford, S.F., et al., "*Weather Forecasting Accuracy for FAA Traffic Flow Management*," The National Academies Press, Washington, DC, 2003, pp. 2.

[2] Klingle-Wilson, D. and J. Evans, "Description of the Corridor Integrated Weather System (CIWS) Weather Products," MIT Lincoln Laboratory, Project Report ATC-317, August, 2005.

[3] Mueller, C.K., et al., "National Convective Weather Forecast Product," *8th Conference on Aviation, Range, and Aerospace Meteorology*, Dallas, Texas, January, 1999.

[4] DeLaura, R.A., M. Robinson, R.F. Todd, and K. MacKenzie, "Evaluation of Weather Impact Models in Departure Management Decision Support: Operational Performance of the Route Availability Planning Tool (RAPT) Prototype," *13th Conference on Aviation, Range, and Aerospace Meteorology*, New Orleans, Louisiana, 2008.

[5] DeLaura, R.A., M. Robinson, M.L. Pawlak, and J.E. Evans, "Modeling Convective Weather Avoidance in En Route Airspace," *13th Conference on Aviation, Range, and Aerospace Meteorology*, New Orleans, Louisiana, 2008.

[6] Rhoda, D.A. and M.L. Pawlak, "The Thunderstorm Penetration/Deviation Decision in the Terminal Area," *8th Conference on Aviation, Range, and Aerospace Meteorology*, Dallas, Texas, 1999.

[7] Rhoda, D.A., et al., "Commercial Aircraft Encounters with Thunderstorms in the Memphis Terminal Airspace," *9th Conference on Aviation, Range, and Aerospace Meteorology*, Orlando, Florida, 2000.

[8] Matthews, M.P. and R.A. DeLaura, "Assessment and Interpretation of En Route Weather Avoidance Fields from the Convective Weather Avoidance Model," *10th AIAA Aviation Technology, Integration, and Operations Conference*, Fort Worth, Texas, 2010.

[9] Garcia, D., "Smoothing of Gridded Data in One and Higher Dimensions with Missing Values," *Computational Statistics and Data Analysis*, vol. 54, 2010, pp. 1167–1178.